Fusion Engineering and Design 202 (2024) 114351

Contents lists available at ScienceDirect

Fusion Engineering and Design

journal homepage: www.elsevier.com/locate/fusengdes

Characterisation of the neutron field for streaming analyses in TT operations at JET

Igor Lengar [a,*], Theodora Vasilopoulou [b], Mariusz Kłosowski [c], Rosaria Villari [d], Bor Kos [a,e], Aljaž Čufar [a], Domen Kotnik [a,f], Luka Snoj [a,f], JET contributors[1]

[a] Jožef Stefan Institute, Jamova cesta 39, 1000 Ljubljana, Slovenia
[b] INRASTES, NCSR Demokritos, 15310 Athens, Greece
[c] Institute of Nuclear Physics Polish Academy of Sciences, 31-342, Krakow, Poland
[d] ENEA, Fusion and Technology for Nuclear Safety and Security, I- 00044, Frascati (Rome), Italy
[e] previously at: Oak Ridge National Laboratory, Oak Ridge, TN, 37831, USA
[f] Faculty of mathematics and physics, University of Ljubljana Jadranska 19, 1000, Ljubljana, Slovenia

ARTICLE INFO

Keywords:
JET
Streaming
TLD
Activation foils
TT
Neutron transport calculations
ADVANTG
MCNP

ABSTRACT

Assessing radiation fields in the biological shield penetrations of fusion reactors is a challenging task. At the Joint European Torus (JET) the neutron field at larger distances from the torus has been calculated and measured. JET operated in 2021–22 with a tritium-tritium plasma and neutronics experiments were performed for validating in a real fusion environment the neutronics codes and nuclear data applied in ITER nuclear analyses. In particular, the fluence of neutrons passing through the penetrations of the JET vacuum vessel and the torus hall was measured and compared with calculations in order to assess the capability of state-of-the-art numerical tools to correctly predict the radiation streaming in large and complex geometries. The neutron fluence was monitored at several locations inside the torus hall at larger distances from the tokamak with activation foils and thermoluminescent detectors. The calculations have been performed in a two-step process using the deterministic code ADVANTG to determine the variance reduction parameters and with MCNP for subsequent calculation of the neutron field with the Monte Carlo method. The paper presents results of calculations and the first comparison to experimentally obtained values.

1. Introduction

JET is, as of 2023, the largest and most powerful operating magnetic confinement fusion device. It is the sole magnetic confinement machine having the capability to operate with a plasma containing tritium and one of only two such devices, next to TFTR [1–3], to have done so in the past. In frame of the DTE2 campaign in 2021, when JET operated using a mixture of deuterium-tritium (DT) plasma, a record-breaking pulse releasing 59 MJ of fusion energy was achieved [4].

Correlated to the DT experiments, JET operated in 2021/22 in the frame of two experimental campaigns for a total of 9 months using a tritium plasma rather than a mixture of D and T. Operation with tritium alone gives opportunities for study of several additional effects including the characteristics of the TT reaction, which produces a continuum of neutron energies rather than a spectrum with a peak. The TT reaction will play an important role in future tokamaks using DT as fuel and is interesting also from a physics point of view [5,6]. The current paper describes the evaluation of the neutron field in the part of the TT campaign denoted C40, Dec. 2020 - July 2021.

The JET torus is a complex machine and has been in operation since 1987 [7]. Since then, numerous smaller and larger components, predominantly experimental equipment, have been placed in the vicinity of the JET machine, forming a very complex environment, as shown in Fig. 1. Due to the inhomogeneous geometry with a large number of ducts and streaming paths through which neutrons can leak from the torus and through the torus hall, it is very challenging to measure or calculate the neutron field outside of the JET vacuum vessel.

One of the projects, carried out during the TT campaign, was the characterization of the neutron field in the torus exterior, subject especially to neutron streaming along penetrations through the torus

* Corresponding author at: Reactor physics division, Jožef Stefan Institute, Jamova cesta 39, Ljubljana, Slovenia.
E-mail address: igor.lengar@ijs.si (I. Lengar).
[1] See ‘Overview of JET results for optimising ITER operation’ by J. Mailloux et al. 2022 Nucl. Fus. 62 04202

https://doi.org/10.1016/j.fusengdes.2024.114351
Received 16 October 2023; Received in revised form 16 February 2024; Accepted 11 March 2024
Available online 29 March 2024

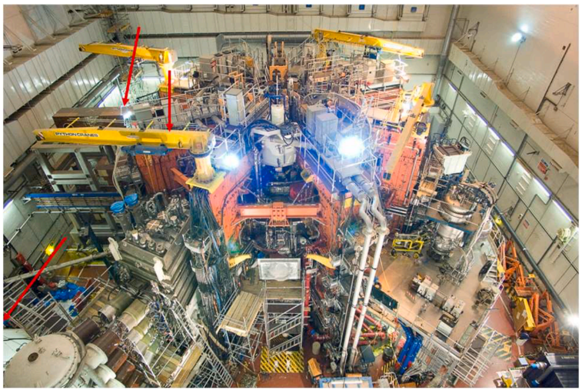

Fig. 1. Complex geometry of JET. Some of the positions of TLDs and activation foils are marked with read arrows (Source: UKAEA).

structure and surrounding equipment. A benchmark evaluation has been performed by comparing experimental measurements with calculations. The emphasis of the present paper is the presentation of calculational results with a first comparison to measurements.

2. Measurements

In several positions inside the torus hall and some positions behind its walls, thermo-luminescent dosimeter (TLD) and activation foil (AF) detectors have been placed. Both types of detectors were positioned inside 25 cm diameter and 25 cm high polyethylene cylinders. The corresponding response function of the TLD detectors resembles the total neutron flux [8,9]. Three dosimetry materials were used as the AF detectors – Co, Ta and Ag foils, making use of the reactions ^{59}Co(n,γ)^{60}Co, ^{181}Ta(n,γ)^{182}Ta and ^{109}Ag(n,γ)^{110m}Ag, respectively. The locations of both types of detectors are presented in Figs. 1 and 2.

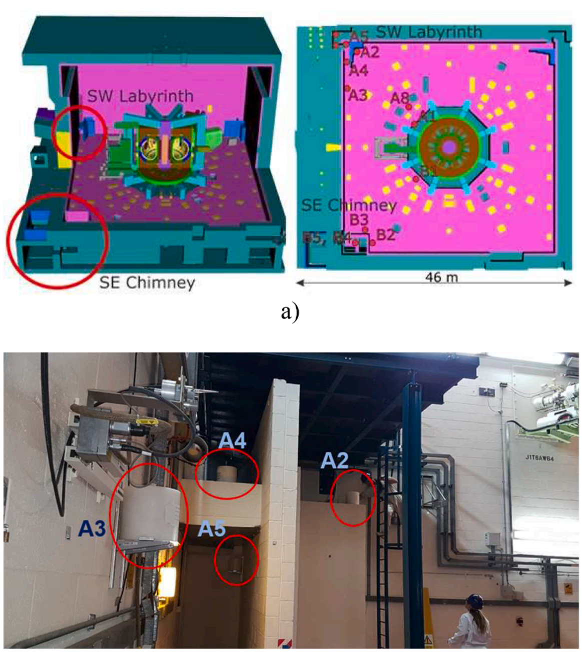

a)

b)

Fig. 2. a) Schematic view of the JET torus pinpointing the detector locations A1 – A8 and B1 – B5, b) picture of detectors A2 – A5 during installation, polyethylene cylinder best visible for the A3 location.

3. Calculations of the neutron field

3.1. Computational model

Several computational models of JET exist. They are constantly updated in accordance with changes to the JET machine and surroundings. The model for use with the Monte Carlo N-Particle (MCNP) code [10] used for the present work is developed by several groups, including CCFE, UU, ENEA and JSI [11]. This model covers the largest part of JET tokamak geometry, including the torus, surrounding structures, torus hall and basement. The cross-section of the model is visible in Fig. 3. Another view of the model is visible also in Fig. 2a.

The level of detail in the MCNP model can be observed from Fig. 3. All major structural components are modelled including the torus hall and details in wall structure, the basement and the roof. However, due to the large number of smaller components and their complexity, not all details are modelled with high accuracy, especially for the experimental and other equipment surrounding the tours as this would not be feasible. An impression of the situation in the surrounding area of the torus is visible in Fig. 4.

All components, surrounding the torus (visible in Figs. 1 and 4) are not explicitly modelled in the MCNP model of JET (pictured in Fig. 3), but in the form of larger cells filled with a homogeneous mixture of materials corresponding to the average of the materials present in reality. The impact of such homogenisation is dependent on the position in which the neutron flux is calculated. It has been estimated in the frame of a neutron calibration project [12] for a position close to the torus, averaged over a larger volume and for a particular neutron energy interval. In that case it was found that the uncertainty did not exceed 10 % for that particular position. In remote locations at larger distances from the plasma, and in a broader energy interval, the impact is estimated to be much larger.

3.2. Calculations

Calculations have been performed in a two-step process by first calculating the variance reduction parameters with the ADVANTG [13] code, based on the results of the discrete ordinates transport code DENOVO [14]. In this way the importance map in terms of geometry and neutron energy is prepared for a particular region of interest, e.g. one of the detectors for the particular spectrum of interest. An example of such an importance map, specifically prepared for the detector location A1, is presented in Fig. 5a. The ADVANTG calculations are performed for

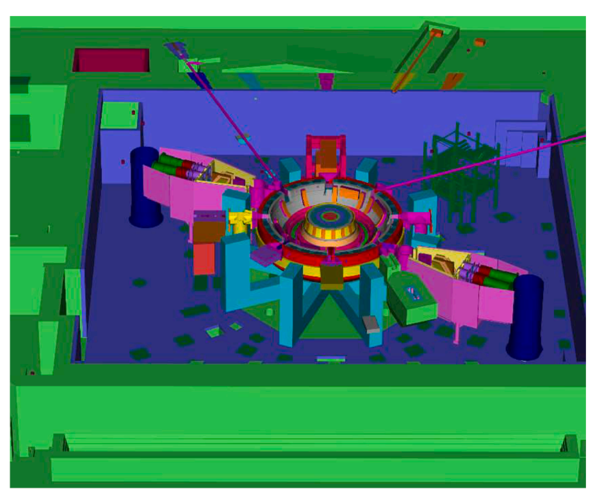

Fig. 3. Schematics of a horizontal cross-section of the MCNP computational model for JET. Outer green colour represents the torus hall walls. The model extends to some structures outside of the torus hall and to the basement (not visible in the figure).

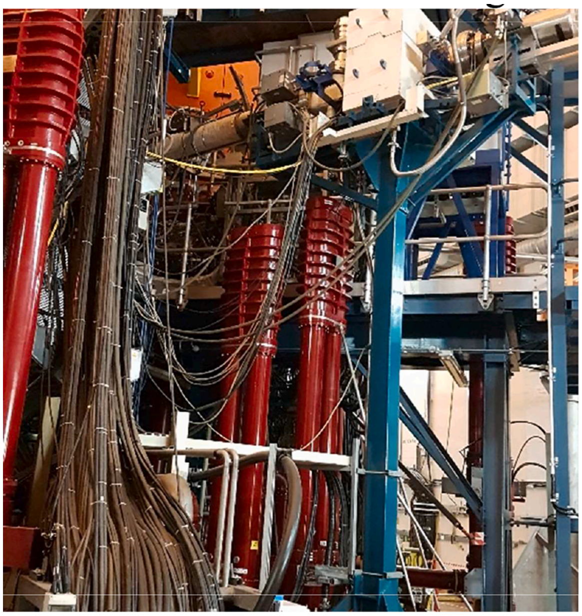

Fig. 4. Detail of the equipment, surrounding the JET torus. An overview of the whole torus is visible in Fig. 1. Some of the equipment is in the MCNP model represented in form of homogeneous cells with an average material composition [11].

optimization to a desired spectrum, i.e. separately for calculation of the total flux at a particular location and for each of the different reaction rates (for the ^{59}Co, ^{181}Ta, ^{109}Ag activation materials). The spatial mesh covered up to 10^7 voxels with varying voxel size ranging from 1 cm^3 close to the region of interest up to 10^4 cm in less important regions of the geometry.

The aim of the second step was to calculate the neutron field using MCNP 6.2 [10] and the FENDL 3.2b [15] nuclear data library. The importance map in the form of space- and energy-dependent weight--windows, as supplied by ADVANTG in the previous step, is used to focus on calculations in the vicinity of the A1 detector, as visible from Fig. 5b. An ADVANTG mesh of up to 10^7 voxels was used with energy resolution optimised for the particular reaction rate. The flux is calculated with the lowest statistical uncertainty in the regions, surrounding the A1 detector and with larger noise in geometry regions less relevant for calculations of the A1 detector flux. In Fig. 5c the relative statistical error of the neutron flux in the whole geometry is presented, with notably smallest value at the A1 location.

3.3. Plasma neutron source

Tritium exclusively has been used as fuel during the TT campaign, however some trace of residual deuterium nuclei from past campaigns was present in the plasma (of the order of less than 1 %). Neutrons were thus produced mainly from 2 reactions:

$$T + T \rightarrow {}^4He + 2 \cdot n$$

$$D + T \rightarrow {}^4He + n$$

The yield of neutrons from the TT reaction was over the course of the TT campaign 59,6 % and the yield of the DT reaction neutrons was 40,4 %. The large percentage of DT neutrons, despite the low concentration of D in the plasma, is a consequence of the two orders of magnitude larger cross-section for the DT reaction with respect to the TT reaction.

The source spectra of neutrons from both reactions, used for the calculations and contributing to the overall source spectrum, are presented in Fig. 6.

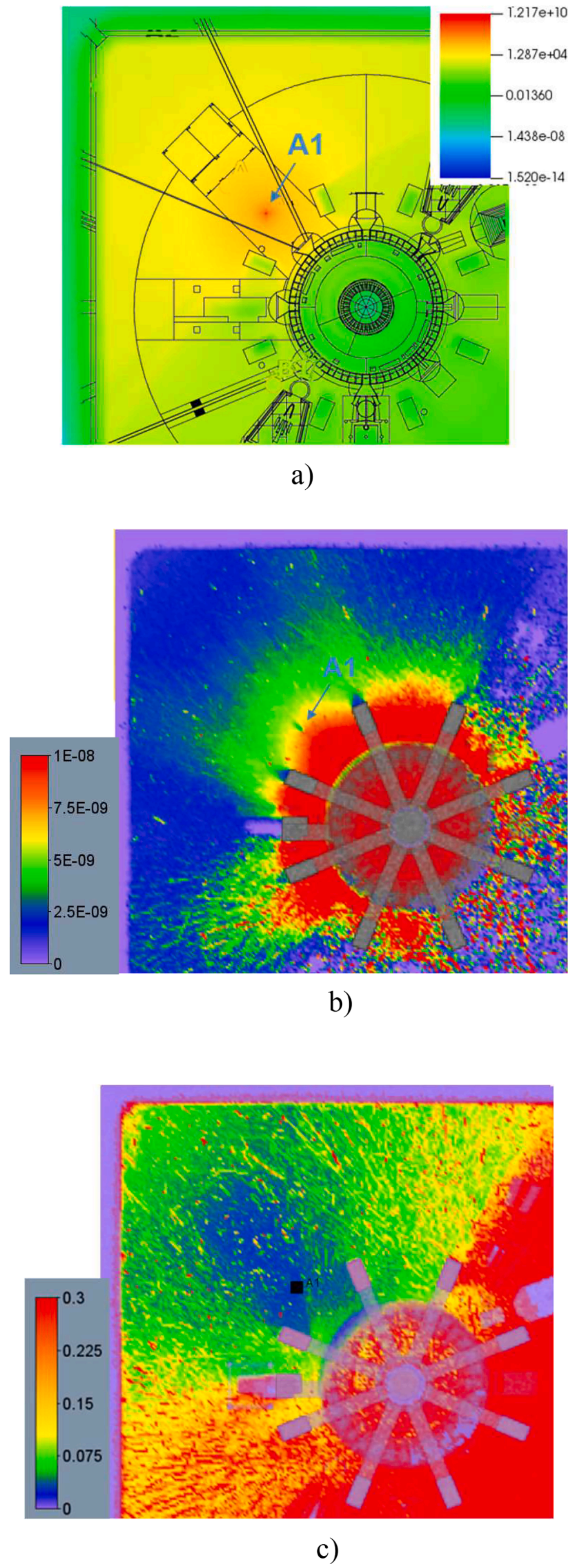

Fig. 5. a) Relative importance map calculated with ADVANTG for the A1 detector location, b) calculated total neutron flux distribution (n/cm^2/source neutron) c) relative error map of total flux distribution (for voxels of dimensions of 15 × 15 × 15 cm^3).

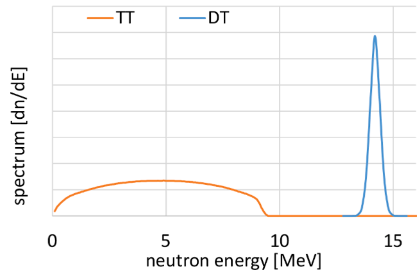

Fig. 6. Spectra of source neutrons, corresponding to the TT and DT reactions in the plasma. The TT reaction produces a continuum of neutron energies [16] while the DT neutrons exhibits a spectrum with a peak at 14.1 MeV.

4. Results

The total number of TT and DT neutrons produced throughout the C40 tritium campaign yielded $8.5 \cdot 10^{18}$ neutrons. The resulting total neutron fluence for the duration of the campaign, calculated for the positions at which TLD detectors were placed, is presented in Fig. 7.

The statistical error of the calculations was low due to the two-stage hybrid approach and was less than 4 % for all detector positions. The error bars present in Fig. 7 are, due to the small statistical error, barely visible.

The calculations for the reaction rates in Co, Ta and Ag samples are presented as the total number of reactions per 1 cm^3 of the sample at a particular activation foil location associated with the total neutron yield in the C40 experimental campaign, i.e. the no. of activation reactions in 1 cm^3 sample during the whole campaign.

4.1. Comparison with experiment – C/E

The experiments were evaluated separately and details of the experimental results will be presented in a separate work. Nevertheless, a comparison with the results of calculations is performed in the present paper.

Comparison of the calculated reaction rates in activation materials (data from Fig. 8) with experiments is presented in Fig. 9 in form of the ratio of the calculated and experimental values, C/E.

The C/E values range from 0.7 to 9. Also presented in Fig. 9 are the combined - measurement and Monte Carlo - statistical uncertainties, dominated by the former. As visible from the figure these uncertainties are for all but one activation foil detector smaller than 25 % and in general much smaller than the deviation of calculations from experiment. This implies that additional uncertainties exist, associated to the great complexity of the studied geometry, one of them is associated with

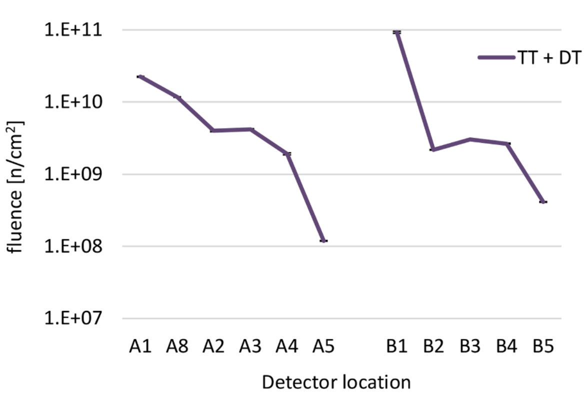

Fig. 7. Total neutron fluence through the C40 experimental campaign, calculated at positions of TLD detectors. Values for positions A (in SW corner of the torus hall) connected with one line and for positions B (in SE corner) with another line.

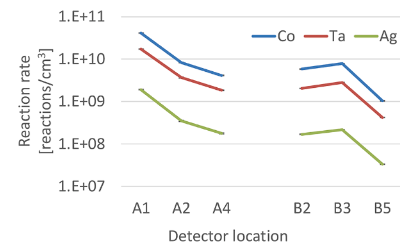

Fig. 8. Reaction rates in Co, Ta, Ag – no. of reactions in 1 cm^3 sample for the total neutron yield of the C40 campaign.

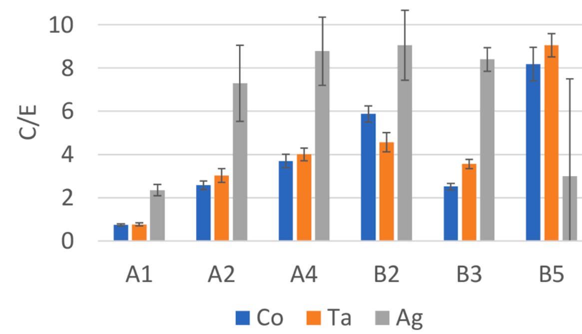

Fig. 9. C/E values for activation detectors. Combined uncertainties - measurement and Monte Carlo statistical uncertainties - are presented.

the simplification of the calculational model. The discrepancies in the C/E ratios for the three foils, in particular the higher values for the Ag foils in most locations as compared to the Co and Ta foil results, could be a consequence of the neutron flux prediction in the energy region of the Ag resonance. It should be noted that the neutron flux at some of the detector locations is, due to the large attenuation in the torus and the surrounding structures, for seven orders of magnitude smaller than the neutron flux close to the plasma source inside the torus. Nevertheless, the presented agreement between calculations and measurements for the TT campaign (C40) is better than it was for the DD campaign, performed at JET in 2019. In that campaign the C/E for AF measurements at the same positions was 0.5 up to 14.

The experimental values for the TLD detectors are under evaluation [9]. The comparison with calculations shows that the ratio of calculation/experiment (C/E) ranges from 0.4 for position A1 to 2.9 for position B5; the A1 is the position closest to the torus, while the detector at the B5 position is placed behind a 40 cm thick wall at the corner of the torus hall (Fig. 2). Again, the agreement between calculation and experiment is better for the same detector locations than in the 2019 DD campaign in which the C/E varied from 0.5 to 6.5 [17].

4.2. Influence of plasma shape

The vertical plasma profile at JET varies between individual pulses and is dependent on several factors [18,19]. The passive TLD and AF detectors measured the fluence corresponding to an average plasma profile over the course of the whole campaign, since they were exposed for the duration of the TT campaign and the integral response was evaluated afterwards.

An estimation of the influence of the plasma profile and corresponding shape of the plasma neutron source on detector response, has nevertheless been performed computationally. In this frame two sets of calculations have been performed, one with a generic plasma profile, i.e. an average profile used for the majority of calculations at JET, and one with a theoretical profile, largely peaked to the centre of the plasma. Visualization of the neutron sources for both profiles is shown in Fig. 10.

Pairs of calculations for a detector position have been performed by

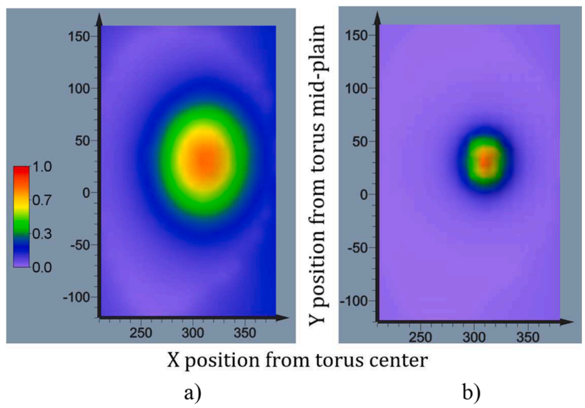

Fig. 10. Plasma neutron source vertical profiles. The colour represents the relative intensity of the TT + DT neutron source as function of position. a) generic (average) neutron source shape, b) neutron source largely peaked towards plasma centre (theoretical profile rather than profile of a specific JET pulse).

using each of the source distributions (shown in Fig. 10) and equal total neutron yields in both cases. The results for the ratio in detector response for three positions are presented in Fig. 11.

It is visible from Fig. 11 that for detector positions A3 and A5, positioned close to torus hall wall, at larger distances from the plasma, no statistically significant difference of detector response is observed between the two cases. In contrast, at position A1, which is closest to the torus, the shape of the plasma has an influence on the result.

It should again be noted that the influence of plasma profile on detector response was not verified experimentally, since only integral measurement values over the whole duration of the TT campaign were available for the TLD and AF detectors.

5. Conclusions

The work on calculations of the neutron field at JET, aimed to support measurements, is presented with emphasis on locations of the thermo-luminescent and activation foil detectors used during the tritium campaign in 2020/21. The neutron fluence at detector positions and the corresponding reaction rates in activation foil materials were calculated with a combination of the MCNP code and the variance reduction code ADVANTG. This hybrid approach was necessary to achieve the low statistical uncertainty in the very demanding geometry of JET and due to the remote location of detectors in which the neutron flux is dominated by neutron streaming.

Comparison of measurements with calculations shows C/E ratios in the range from 0.5 to 7 for the responses of TLDs and AFs, however these measurements are in conditions in which the degradation of the neutron flux from plasma to detector positions amounts to seven orders of magnitude. In gross, the C/E values show an improvement compared to the preceding DD campaign. The largest uncertainty in the results is attributed to the difficulty in modelling the complex geometry of the JET torus.

Computational study of the sensitivity of results with respect to changes in the plasma neutron source profile showed an influence on results only for the detectors closer to the plasma.

It should be emphasized that benchmark evaluations with the comparison of measurements and the state-of-the-art calculations are a very valuable tool, showing the limits of calculations. Such comparison in large tokamak environment is especially important since planning of future tokamaks like ITER and DEMO is, at present, limited to large amounts of calculations only.

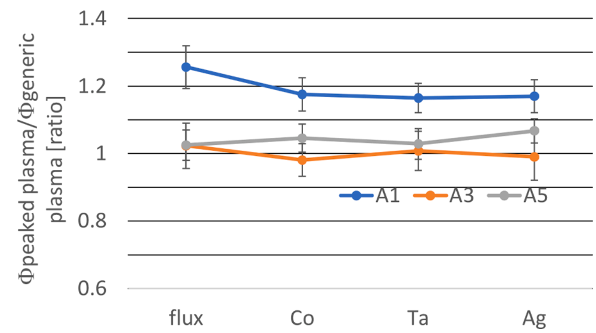

Fig. 11. Total neutron fluence and reaction rates at positions A1, A3, A5 – presented is the ratio of results with a peaked plasma neutron source profile vs. results with the generic source profile.

CRediT authorship contribution statement

Igor Lengar: Conceptualization, Methodology, Writing – original draft, Writing – review & editing. **Theodora Vasilopoulou:** Data curation, Formal analysis, Investigation. **Mariusz Kłosowski:** Data curation, Formal analysis, Investigation. **Rosaria Villari:** Conceptualization, Methodology, Supervision. **Bor Kos:** Methodology, Validation. **Aljaž Čufar:** Methodology, Validation. **Domen Kotnik:** Methodology, Writing – review & editing. **Luka Snoj:** Supervision, Validation.

Declaration of competing interest

The authors declare that they have no known competing financial interests or personal relationships that could have appeared to influence the work reported in this paper.

Data availability

Data will be made available on request.

Acknowledgments

The authors acknowledge the support of the Slovenian Ministry of Education, Science and Sport (project codes P2–0405 Fusion technologies; P2–0073 Reactor physics). This work has been carried out within the framework of the EUROfusion Consortium, funded by the European Union via the Euratom Research and Training Programme (Grant Agreement No 101052200 — EUROfusion). Views and opinions expressed are however those of the author(s) only and do not necessarily reflect those of the European Union or the European Commission. Neither the European Union nor the European Commission can be held responsible for them.

References

[1] J. Mailloux, et al., Overview of JET results for optimising ITER operation, Nucl. Fusion 62 (2022) 042026, https://doi.org/10.1088/1741-4326/ac47b.
[2] M. Nocente, V. Kiptily, M. Tardocchi, et al., Fusion product measurements by nuclear diagnostics in the Joint European Torus deuterium-tritium 2 campaign, Rev. Sci. Instruments 93 (2022) 093520, https://doi.org/10.1063/5.0101767.
[3] J.D. Strachan, et al., TFTR DT experiments, Plasma Phys. Control. Fusion 39 (1997) B103, https://doi.org/10.1088/0741-3335/39/12B/008.
[4] https://euro-fusion.org/eurofusion-news/european-researchers-achieve-fusion-energy-record/.
[5] https://euro-fusion.org/eurofusion-news/tritium-campaign-prepares-jet-for-the-real-deal/.
[6] I. Lengar, et al., Activation material selection for multiple foil activation detectors in JET TT campaign, Fusion Engineering and Design, Part B 136 (2018), https://doi.org/10.1016/j.fusengdes.2018.04.052.
[7] https://ccfe.ukaea.uk/programmes/joint-european-torus/.
[8] T. Vasilopoulou, Report on analyses of TT and DT neutron flux measurements with Activation Foils, Eurofusion (2023). https://idm.euro-fusion.org/default.aspx?uid=2Q9RVJ.

[9] M. Klosowski, Report on analysis of TT and DT neutron flux measurements with TLDs and calibration at high doses, Eurofusion (2023). https://idm.euro-fusion.org/default.aspx?uid=2QBLX3.
[10] MCNP® User's manual, Code Version 6.2, Los Alamos National Laboratory report LA-UR-17-29981 (2017).
[11] P. Batistoni, et al., Calibration of neutron detectors on the Joint European Torus, Rev. Sci. Instrum. 88 (2017) 103505, https://doi.org/10.1063/1.4991780.
[12] A. Čufar, P. Batistoni, S. Conroy, Z. Ghani, I. Lengar, S. Popovichev, B. Syme, Ž. Štancar, L. Snoj, Situ neutron yield calibrations at the joint European Torus, Fusion Science and Technology 74 (4) (2018) 370–386, https://doi.org/10.1080/15361055.2018.1475163.
[13] S.W. Mosher, et al., ADVANTG An Automated Variance Reduction Parameter Generator, Rev.1, Oak Ridge National Laboratory and United States. Department of Energy and United States. Department of Energy. Office of Scientific and Technical Information, (2015).
[14] T.M. Evans, A.S. Stafford, R.N. Slaybaugh, K.T. Clarno, Denovo: a new three-dimensional parallel discrete ordinates code in SCALE, Nucl Technol 171 (2) (2010) 171–200.
[15] R.A. Forrest, et al., FENDL-3 library, IAEA (2012). INDC(NDS)-0628.
[16] L.N. Bogdanova, D.L. Demin, V.V. Filchenkov, Study of the mechanism of muon-catalyzed T + T fusion reaction, Phys. Atomic Nuclei 78 (1) (2015), https://doi.org/10.1134/S1063778815010020.
[17] B. Kos, et al., Analysis of DD, TT and DT neutron streaming experiments with the ADVANTG code. EPJ Web of Conferences, EDP Sciences, 2020, p. 02003, vol. 225.
[18] A. Žohar, et al., Modelling of plasma gamma ray sources in large tokamaks, Fusion Eng. Design 163 (2021), https://doi.org/10.1016/j.fusengdes.2020.112158.
[19] Ž. Štancar, Generation of a plasma neutron source for Monte Carlo neutron transport calculations in the tokamak JET, Fusion Eng. Design 136 (2018), https://doi.org/10.1016/j.fusengdes.2018.04.065. Part B.